How to cite: *Angew. Chem. Int. Ed.* **2021**, *60*, 21583–21591
International Edition: doi.org/10.1002/anie.202107599
German Edition: doi.org/10.1002/ange.202107599

Perovskites | Very Important Paper

# Fluoride Chemistry in Tin Halide Perovskites

*Jorge Pascual[+],* Marion Flatken[+], Roberto Félix, Guixiang Li, Silver-Hamill Turren-Cruz, Mahmoud H. Aldamasy, Claudia Hartmann, Meng Li, Diego Di Girolamo, Giuseppe Nasti, Elif Hüsam, Regan G. Wilks, André Dallmann, Marcus Bär, Armin Hoell, and Antonio Abate**

***Abstract:*** *Tin is the frontrunner for substituting toxic lead in perovskite solar cells. However, tin suffers the detrimental oxidation of $Sn^{II}$ to $Sn^{IV}$. Most of reported strategies employ $SnF_2$ in the perovskite precursor solution to prevent $Sn^{IV}$ formation. Nevertheless, the working mechanism of this additive remains debated. To further elucidate it, we investigate the fluoride chemistry in tin halide perovskites by complementary analytical tools. NMR analysis of the precursor solution discloses a strong preferential affinity of fluoride anions for $Sn^{IV}$ over $Sn^{II}$, selectively complexing it as $SnF_4$. Hard X-ray photoelectron spectroscopy on films shows the lower tendency of $SnF_4$ than $SnI_4$ to get included in the perovskite structure, hence preventing the inclusion of $Sn^{IV}$ in the film. Finally, small-angle X-ray scattering reveals the strong influence of fluoride on the colloidal chemistry of precursor dispersions, directly affecting perovskite crystallization.*

## Introduction

Metal halide perovskite materials have shown enormous potential for the processing of efficient and stable photovoltaics.[1] However, the dominant type of perovskite solar cells (PSCs) are based on lead, a metal whose toxicity and environmental hazard can hinder its commercial application in numerous fields.[2] The lead threat pushed the scientific community to develop lead-free perovskite materials to maintain excellent photovoltaic performance while avoiding environmental risks. In this sense, tin halide perovskites are the best candidate to replace the dominant lead-based counterparts.[3,4] Nevertheless, these materials face some difficulties related to their inherent physicochemical characteristics.[5] The most important one is the ease with which $Sn^{II}$ oxidizes into $Sn^{IV}$ species, leading to the substantial decline in the performance through the undesirable formation of electron traps and p-doping of the material.[6] Previous studies have reported many origins of this oxidation, such as the solvent,[7,8] the processing conditions[9] or even spontaneously through disproportionation in tin-poor environments.[10] Stopping this oxidation is one of the requirements to achieve efficient and stable tin halide PSCs. For this reason, several trials have been made tackling the oxidation of $Sn^{II}$. These include the use of new solvent systems to avoid the oxidation by dimethyl sulfoxide (DMSO),[11] employing reducing agents to eliminate the content of $Sn^{IV}$, such as metallic Sn powder[12] or hypophosphorous acid[13] or introducing additives for alleviating the formation of $Sn^{IV}$, like the ever-present $SnF_2$.[6,14]

$SnF_2$ has achieved remarkable success as an additive in the tin halide perovskite field. Since its first use in PSCs by Kumar and co-workers,[15] it has been proven over time as an imperative to achieve good results (Figure 1a). There is barely any good cell performance report without $SnF_2$; exceptional cases use $SnCl_2$,[16,17] which may behave similarly to $SnF_2$, or 2D materials, which are another popular strategy for processing tin-based perovskites.[18–20] The appeal of $SnF_2$ in the community is such that the number of studies not using it (nor $SnCl_2$) quickly stagnated over the years, being in 2020 below 10% of the total publications on tin halide perovskites

[*] Dr. J. Pascual,[+] M. Flatken,[+] Dr. R. Félix, G. Li, M. H. Aldamasy, Dr. C. Hartmann, Dr. M. Li, E. Hüsam, Dr. R. G. Wilks, Prof. M. Bär, Dr. A. Hoell, Prof. A. Abate
Helmholtz-Zentrum Berlin für Materialien und Energie GmbH
Hahn-Meitner-Platz 1, 14109 Berlin (Germany)
E-mail: jorge.mielgo@helmholtz-berlin.de
antonio.abate@helmholtz-berlin.de

Dr. S.-H. Turren-Cruz
Institute of Advanced Materials (INAM), Jaume I University
Castelló de la Plana (Spain)

M. H. Aldamasy
Egyptian Petroleum Research Institute
Cairo (Egypt)

Dr. D. Di Girolamo, Dr. G. Nasti, Prof. A. Abate
Department of Chemical, Materials and Production Engineering, University of Naples Federico II
80125 Naples (Italy)

Dr. A. Dallmann
Institut für Chemie, Humboldt Universität zu Berlin
Brook-Taylor-Str. 2, 12489 Berlin (Germany)

Prof. M. Bär
Department of Chemistry and Pharmacy, Friedrich-Alexander Universität Erlangen-Nürnberg (FAU)
91058 Erlangen (Germany),
and
Department for X-ray Spectroscopy at Interfaces of Thin Films, Helmholtz-Institute Erlangen-Nürnberg for Renewable Energy (HI-ERN)
12489 Berlin (Germany)

[+] These authors contributed equally to this work.

Supporting information and the ORCID identification number(s) for the author(s) of this article can be found under: https://doi.org/10.1002/anie.202107599.

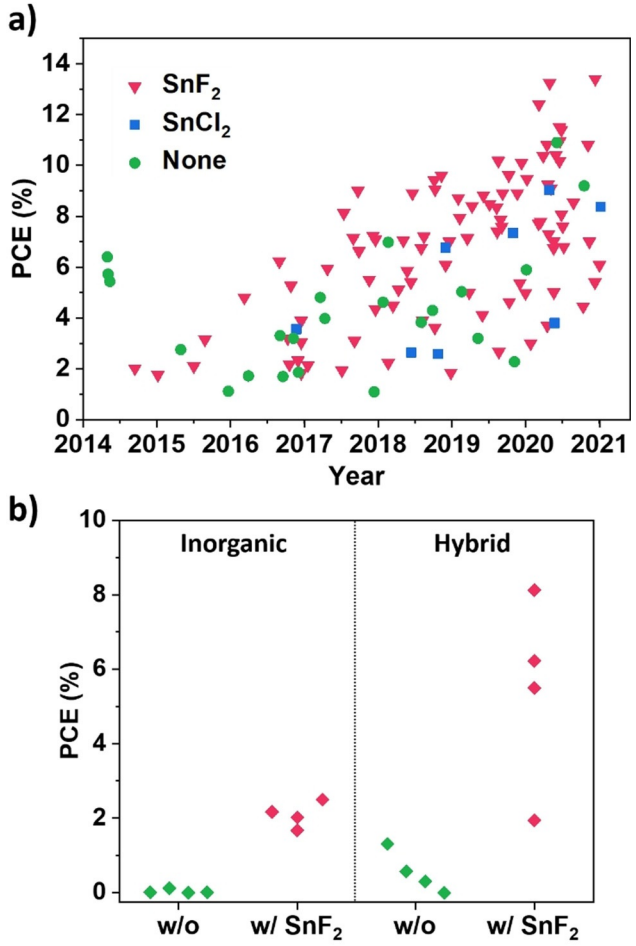


***Figure 1.*** a) Highest PCE reported in tin halide perovskites literature containing solar cell data using $SnF_2$, $SnCl_2$, or none of them, ordered by date until Jan. 2021. b) Comparison of solar cell performance improvement in inorganic and hybrid tin halide perovskites before and after the addition of $SnF_2$, extracted from the studies in literature in which the comparison is made.[15,21–27]

in that year (Figure S1). Its success lies mainly in the impossibility to obtain photovoltaic behaviour in the solar cells fabricated without it. In Figure 1b, we collected data from studies in which solar cells were made with and without $SnF_2$.[15,21–27] The improvement in efficiency for both inorganic and hybrid tin halide perovskites is enormous, with negligible efficiency for the $SnF_2$-free cases. One of the most reported improvements is the better substrate coverage and film morphology obtained with $SnF_2$,[22,25,28] which implies that $SnF_2$ affects the film crystallization, a factor that remains unexplored. Nevertheless, its addition needs to be controlled, as a too-high content of $SnF_2$ is reported to induce phase separation.[22,25,28] The other most explored effect is the ability of $SnF_2$ to reduce the formation of $Sn^{IV}$ and its related defects, with the reported benefits usually being reduced recombination[24] and a blue shift of the absorption onset.[24,29,30] Besides, Savill and co-workers found out that even low amounts of $SnF_2$ are sufficient to positively impact mitigating $Sn^{IV}$ formation in tin/lead perovskites.[29] This effect on oxidation suppression could originate from introducing a Sn-rich environment, reducing Sn vacancies.[10] This interpretation has been proposed already in the first use of this additive by Kumar et al.[15] However, the question of what fluoride is doing and why we do not provide the Sn-rich environment simply with a higher $SnI_2$ ratio in respect to FAI remains unanswered. Related to this, other $Sn^{II}$ species that could provide the same beneficial effect were already discussed by Yokoyama et al.[31] Using $SnI_2$ excess also led to good results in one of the first studies on inorganic tin halide perovskites.[32]

Overall, reports in literature consistently lead to the same results: $SnF_2$ has a critical positive influence on the formation of high-quality $ASnX_3$ (where A = methylammonium ($MA^+$), formamidinium ($FA^+$) and $Cs^+$, and X = $Cl^-$, $Br^-$ and $I^-$) films and holds a particular role in the stability of these materials against their oxidation to $Sn^{IV}$. These two possibly related aspects are the key to $SnF_2$ being the predominant, most robust additive in the tin-based perovskite field. While there has been extensive exploration of the impact and functioning of $SnF_2$ in these thin films, the chemical mechanism and influence in the processing are entirely unknown. Introducing an exact Scheme of its working procedure remains a must in the field. This move would open the door to optimized application and help identify new additives in the future.

In this work, we explain the origin of the beneficial effects of $SnF_2$ in the processing and stability to oxidation of tin halide perovskites by studying the chemistry of fluoride in these solutions. Using a combination of complementary solution and film characterization techniques, we propose that the role of $SnF_2$ is not limited to the resulting thin film but also affects the precursor solution properties critically and hence their processing. The study of the solution chemistry of fluoride in formamidinium (FA)-based $FASnI_3$ precursor solutions by $^{119}$Sn- and $^1$H-NMR revealed a strongly predominant affinity of the fluoride anion for $Sn^{IV}$ over $Sn^{II}$. With the help of hard X-ray photoelectron spectroscopy (HAXPES) analysis, we show how $SnF_2$ increases the $Sn^{II}$ content in perovskite samples, an indication that $Sn^{IV}$ is partially prevented from being incorporated in the perovskite film. Meanwhile, small-angle X-ray scattering (SAXS) enables an understanding of how fluoride anion modifies perovskite subunits' interaction in solution, generating improved homogeneous crystal growth conditions. Furthermore, experiments with other fluoride species and $SnCl_2$ prove that these effects are not exclusive to $SnF_2$. Thus, the chemistry of a hard Lewis base like fluoride, combined with the Sn-rich environment, make $SnF_2$ a highly suitable additive for processing tin halide perovskites.

## Results and Discussion

Previous works concluded that $SnF_2$ could reduce the $Sn^{IV}$ content in solutions and films.[14,30] However, the redox activity cannot explain the multiple effects of $SnF_2$ in $ASnX_3$ perovskites entirely. Therefore, we postulated that $SnF_2$ must be involved in a different type of chemical reaction. In the early stages of tin halide perovskites development, it was thought that a yellow color for the solution implied the elimination of $Sn^{IV}$ through its reduction by $SnF_2$.[28] Using

  

NMR, we uncover that $Sn^{IV}$ and $SnF_2$ do not undergo a redox reaction, but a simple ligand exchange reaction, producing colorless $SnF_4$ in solution. In this regard, we prepared $FASnI_3$ precursors solutions with and without $SnF_2$ and $Sn^{IV}$ to investigate their signature chemistry. $^{119}$Sn-NMR is sensitive to Sn nuclei in different electronic environments, allowing to identify of the Sn species existing in the solution, including other oxidation states of the same nucleus.

Figure 2a depicts the change in color from orange to the pale yellow of a 1 M $FASnI_3$ solution in DMSO after the addition of $SnF_2$. Following the same method, we added $SnF_2$ to a $Sn^{IV}$-containing solution after being aged by heating at 100 °C for 3 h. Saidaminov et al. and we recently described that this thermal treatment promotes $Sn^{II}$ oxidation in DMSO solutions.[7,8] The color of the aged solution goes from an intense red to a pale yellow to that of the fresh sample. Unlike the fresh solution, we know that certain content of $Sn^{IV}$ is present for the aged one. Still, the color after $SnF_2$ for the aged solution is the same as for the fresh solution, suggesting that the characteristics and species in the solution are changing, no matter the $Sn^{IV}$ content.

$^{119}$Sn-NMR of the fresh solution indicates neither elimination nor formation of $Sn^{IV}$, even though its color changes to pale yellow (Figure 2b). However, we observe the $Sn^{II}$ shielding resulting in a chemical shift change from −574 ppm to −604 ppm. Regarding the $Sn^{II}$ species ($SnI_2$ and $SnF_2$), they cannot be differentiated in solution, as they show up in a single signal belonging to the average electronic environment of $Sn^{II}$ in solution. In this sense, the addition of increasing amounts of $SnF_2$ shifts the $Sn^{II}$ peak to lower chemical shift values in a fairly linear manner, as we show in Figure S2. In contrast to the fresh solution, the aged $FASnI_3$ solution showed the expected $SnI_4$ signal at −2025 ppm. After the addition of $SnF_2$, this peak disappeared, and a new quintuplet rose at −770 ppm (Figure 2c). To identify the newly formed species, we measured solutions in DMSO of $SnI_2$, $SnI_4$, $SnF_2$ and $SnF_4$ by $^{119}$Sn-NMR (Figures 2d), indicating that the species corresponds to $SnF_4$. This result, therefore, implies that $SnF_2$ cannot reduce $Sn^{IV}$ from an oxidized sample. Instead, it coordinates $Sn^{IV}$ via a ligand exchange reaction between the fluorides from $Sn^{II}F_2$ and the iodides from oxidized $Sn^{IV}I_4$ [Eq. (1)]:

$$Sn^{IV}I_4 + 2\,Sn^{II}F_2 \rightarrow Sn^{IV}F_4 + 2\,Sn^{II}I_2 \quad (1)$$

As shown in Figure 2e, a colorless solution comprising $SnI_2$ and $SnF_4$ presented both mixed species' signals in NMR. However, mixing $SnF_2$ and $SnI_4$, the resulting NMR species observed were $SnI_2$ and $SnF_4$. Consequently, the complexation selectivity of fluoride ions towards $Sn^{IV}$ is absolute (Figure 2f). This can be easily explained by the "hard and soft (Lewis) acids and bases" (i.e. HSAB theory) nature of the different solution species. Fluoride is a small, non-polarizable, very electronegative anion that shows a stronger affinity for a cation of a similar nature, that is, $Sn^{IV}$, which is smaller and more electronegative than its reduced analogue $Sn^{II}$. This hard Lewis base character of fluoride anions was already applied in previous works on lead halide perovskites, owing to its ability to passivate vacancies due to their strong bonds with

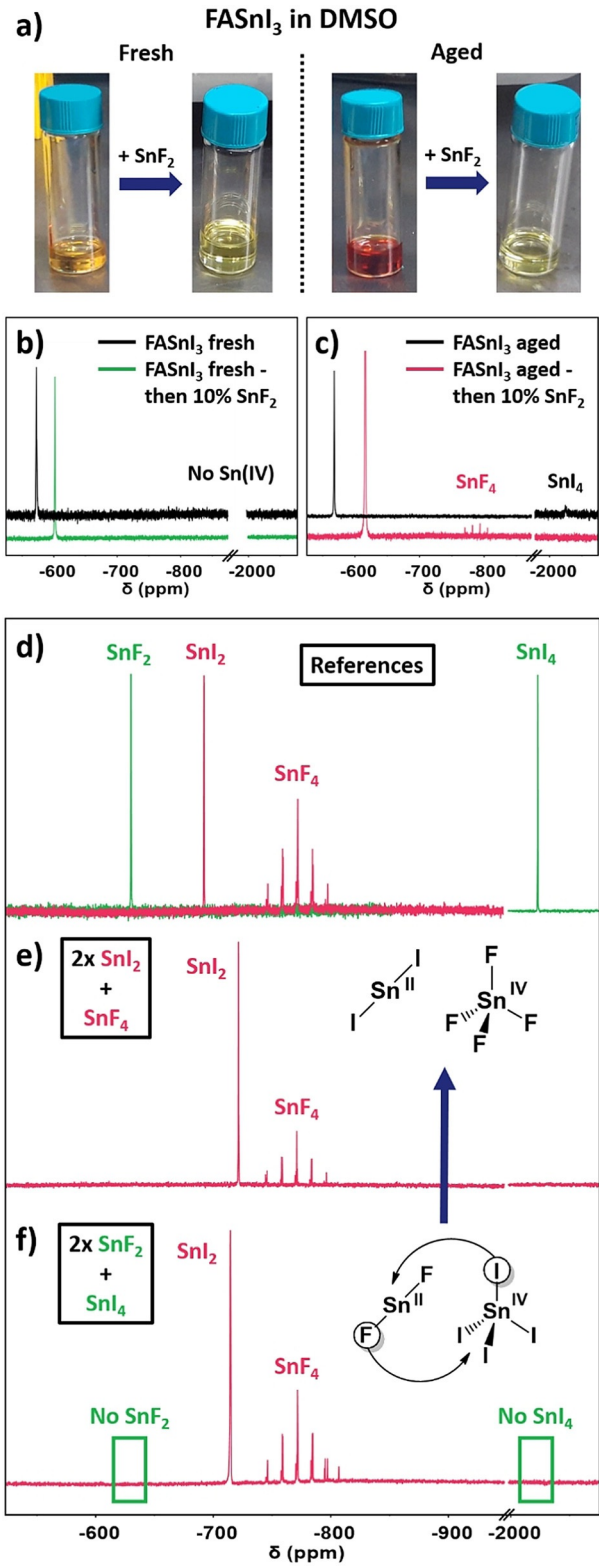


*Figure 2.* a) Pictures of fresh and aged $FASnI_3$ solutions in DMSO before and after the addition of $SnF_2$ in 10 mol%; the respective $^{119}$Sn-NMR spectra of b) fresh and c) aged solutions; d) $^{119}$Sn-NMR spectra of $SnF_2$, $SnI_2$, $SnF_4$ and $SnI_4$ in DMSO. Further information about solution preparation in Figure S3. $^{119}$Sn-NMR spectra and solution pictures of the mixing of e) 2× $SnI_2$ and $SnF_4$ and f) 2× $SnF_2$ and $SnI_4$. The signal magnification was adapted accordingly for illustrative purposes.

  

$Pb^{II}$.[33] In the present case, we find that fluoride's role is connected to $Sn^{IV}$ complexation. Simultaneously, the passivation of undercoordinated $Sn^{II}$ in the thin film should not be excluded.

The only appearance so far of this species can be found in Nakamura and co-workers' work. The authors use an $SnF_2$-selective reducing agent to effectively generate $Sn^0$ nanoparticles to scavenge $Sn^{IV}$ from the solution.[34] Even though there is no particular discussion on the formation of $SnF_4$ and it does not affect their mechanism, the $^{119}$Sn-NMR spectra provided in their work show the signal, also a multiplet, corresponding to $SnF_4$ at approximately −750 ppm when adding $SnF_2$ to a $Sn^{IV}$-containing solution. This different multiplicity that the $SnF_4$ signal presents in $^{119}$Sn-NMR compared to the rest of the Sn species can be explained by coupling between the Sn and halide nuclei. $SnF_4$ has four chemically equivalent $^{19}$F-spins (each with spin 1/2) to couple with, which results in a perfect quintuplet as observed. In this sense, we would expect to observe a triplet for $SnF_2$. However, the four coordination sites are not saturated in $SnF_2$, and, thus, there is an exchange with other impurity-related compounds, such as water. Birchall and Dénès found the same behaviour. They claimed that the missing coupling between $^{19}$F and $^{119}$Sn is due to the exchange between different hydrated species of $SnF_2$.[35] Our samples contain water since non-anhydrous [$D_6$]DMSO was used as a solvent for the NMR experiments, therefore agreeing with the previously reported experiences. For other species, no splitting occurs since chloride, bromide, and iodide do not have NMR-active nuclei in significant amounts or with detectable line widths.

This affinity of fluorides towards $Sn^{IV}$ can have several important implications that may reduce $Sn^{IV}$ content in the final film. For instance, the strong preference for $Sn^{IV}$ means that fluorides could complex it as soon as it is generated, whether from $O_2$ in the environment or DMSO-driven oxidation.[7,8,11] In fact, one should think if $SnF_2$ would be as valuable for other solvents as in DMSO, as fluorides could be critical in sequestrating $Sn^{IV}$ as soon as it is oxidized by this solvent, making it less harmful. The conversion of $SnI_4$ into $SnF_4$ will also prevent the $SnI_4$-driven degradation pathways recently described by Lanzetta et al.[36] Furthermore, the selective complexation of $Sn^{IV}$ as $SnF_4$ may hinder its ability to form any perovskite-like complex in solution. It has been widely reported for $SnF_2$ that this material's excess tends to undergo phase separation.[22,25,28] Conclusively, if $Sn^{IV}$ is retained as $SnF_4$, it would be challenging to incorporate this form into the perovskite lattice. Instead, it would be displaced to grain boundaries or even removed from the film. As a result, the point defects resulting from incorporated $Sn^{IV}$ in the perovskite lattice can be significantly reduced. To prove this, we compared the different $Sn^{IV}$ species' ability to coordinate with FAI by analyzing the $^1$H-NMR of these solutions. Figure S4 shows how all $SnI_2$ ($FASnI_3$), $SnF_4$ and $SnI_4$ cause the splitting of the FAI aminic protons, pointing out a certain degree of interaction between the species. However, the signals for all N- and C-attached protons are slightly shielded in the $FASnI_3$ solution (where the formation of perovskite adducts in solution occurs), whilst for the case of $SnF_4$, there is no shielding, suggesting that the interaction of $SnF_4$ species might have a lower affinity towards perovskite precursors. Moreover, the shift is very pronounced for $SnI_4$, which might imply strong coordination with FAI and an increased ability to get incorporated in the perovskite, resulting in adverse consequences for the photovoltaic properties of the films.

The impact of $Sn^{IV}$ complexation by fluoride in the preparation of $FASnI_3$ on the Sn chemical environment in the resulting films was investigated via HAXPES. For that, 10 mol% of $SnF_2$, $SnI_2$, $SnF_4$ and $SnI_4$ was deliberately added to $FASnI_3$ perovskite precursor solutions. Figure 3 presents HAXPES spectra of the Sn 4d energy region of $FASnI_3$

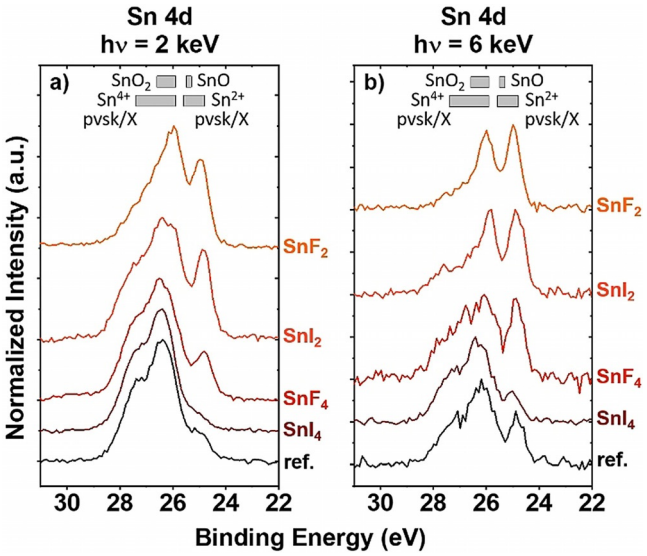


***Figure 3.*** HAXPES spectra of Sn 4d core levels of $FASnI_3$ films prepared without ("ref.") and with 10 mol% of $SnF_2$, $SnI_2$ (excess), $SnF_4$ and $SnI_4$, measured using a) 2 keV and b) 6 keV excitation and normalized to maximum intensity (after background subtraction). The used additives are labelled next to the corresponding spectra. The grey-filled boxes denote the binding energy of Sn $4d_{5/2}$ of Sn-based reference compounds reported in the literature.[30,37–39] "$Sn^{2+}$ pvsk/X" stands for perovskite (tin halide salt) compounds with various $ASnX_3$ ($SnX_2$) compositions. "$Sn^{4+}$ pvsk/X" stands for perovskite (organotin halide) compounds with various $ASnX_6$ ($Ph_3SnX$) compositions.

samples prepared with and without various additives, measured with excitation energies of 2 keV and 6 keV, respectively. It is possible to vary the probing depths of the HAXPES measurements using different excitation energies, that is, the 2 keV data is more surface-sensitive than the 6 keV data (see methods section). The spectra shown in Figure 3 do not exhibit a line shape that resembles a single Sn $4d_{5/2}$-$4d_{3/2}$ doublet peak (i.e., with a $3:2 = 4d_{5/2}:4d_{3/2}$ area ratio and a $4d_{5/2}$-$4d_{3/2}$ spin-orbit separation of ≈1.1 eV);[30,40] this is a clear indication that spectral contributions from more than one Sn chemical species are detected. Overall, the Sn 4d spectra suggest substantial contributions in the binding energy (BE) regions (24.9 ± 0.1) eV and (26.2 ± 0.2) eV, corresponding to values reported in the literature for Sn $4d_{5/2}$ of Sn-based perovskite/halide and oxide reference compounds with Sn being in $Sn^{2+}$ and $Sn^{4+}$ environments, respectively.[30,37–39] Because the Sn 4d BE values of $Sn^{2+}$ (SnO) and $Sn^{4+}$

  

($SnO_2$) oxide compounds are energetically overlapping with the respective Sn environments expected to be present in the sample set (i.e., $FASnI_3$ and the different Sn-based additives) and O-related lines were detected in the HAXPES measurements, the Sn 4d spectra in Figure 3 likely contain Sn oxide derived spectral features and thus consist of more than two doublet peaks. Comparing the spectra in Figure 3a with the spectra in Figure 3b demonstrates that the high BE $Sn^{4+}$-related features are more prominent in the 2 keV measurements than in the 6 keV, which indicates an increased prevalence of the $Sn^{4+}$ related species (in the form of $SnO_2$ or $SnX_4$) near the surface of samples than deeper within their bulk. However, significant differences in the line shape of the spectra for a given excitation set reveal pronounced changes in the Sn chemical environment of the investigated samples concerning the presence/absence and kind of additives during processing. The spectra of samples with additives containing $Sn^{2+}$ or $F^-$ display a significant increase in the low BE $Sn^{2+}$-related signal. This finding seems to be in line with the NMR results described above, that capturing $Sn^{IV}$ in the form of fluorinated species prevents its incorporation in the films. However, the observed variability of properties at the surface of the samples associated with handling conditions of the Sn-based perovskite samples (as has been already reported,[30] and further discussed in Supporting Information, see Figure S5) prevents the present interpretation of the HAXPES results from reaching further conclusions on the impact of individual additives with statistical certainty.

As depicted previously in Figure 2a, we attribute the color change of $FASnI_3$ in DMSO to the change in solution properties and not to the $Sn^{IV}$ content. Nevertheless, it is crucial to understand the underlying reasons that led to this change, as we expect it to exhibit a decisive influence on the crystallization dynamics.

Here, we perform transmission small-angle X-ray scattering (SAXS) to reveal the effect of $SnF_2$ on the perovskite precursors in solution. Thereby, a proposed nucleation mechanism indicates that the use of $SnF_2$ promotes homogeneously distributed growth, yielding improvements in the overall crystal quality. Using the SAXS instrument at BESSY II at X-ray energies of 8 keV and 10 keV ($\Delta E/E = 2 \times 10^{-4}$), we cover a $q$-range from 0.05 to 8.5 $nm^{-1}$ (size range: 209.4–0.74 nm). Figure 4a compares the SAXS scattering curve of a plain $FASnI_3$ solution in DMSO with $FASnI_3$ containing $SnF_2$. At first sight, the comparison does not show significant variations.

Nevertheless, by applying a model fit using the software SASfit©,[41] which offers several different form and structure factors describing various shapes of particles and their interaction, small changes regarding the particle interplay in the high $q$-region can be observed. Here, however, interpretation requires particular precaution since we are already in

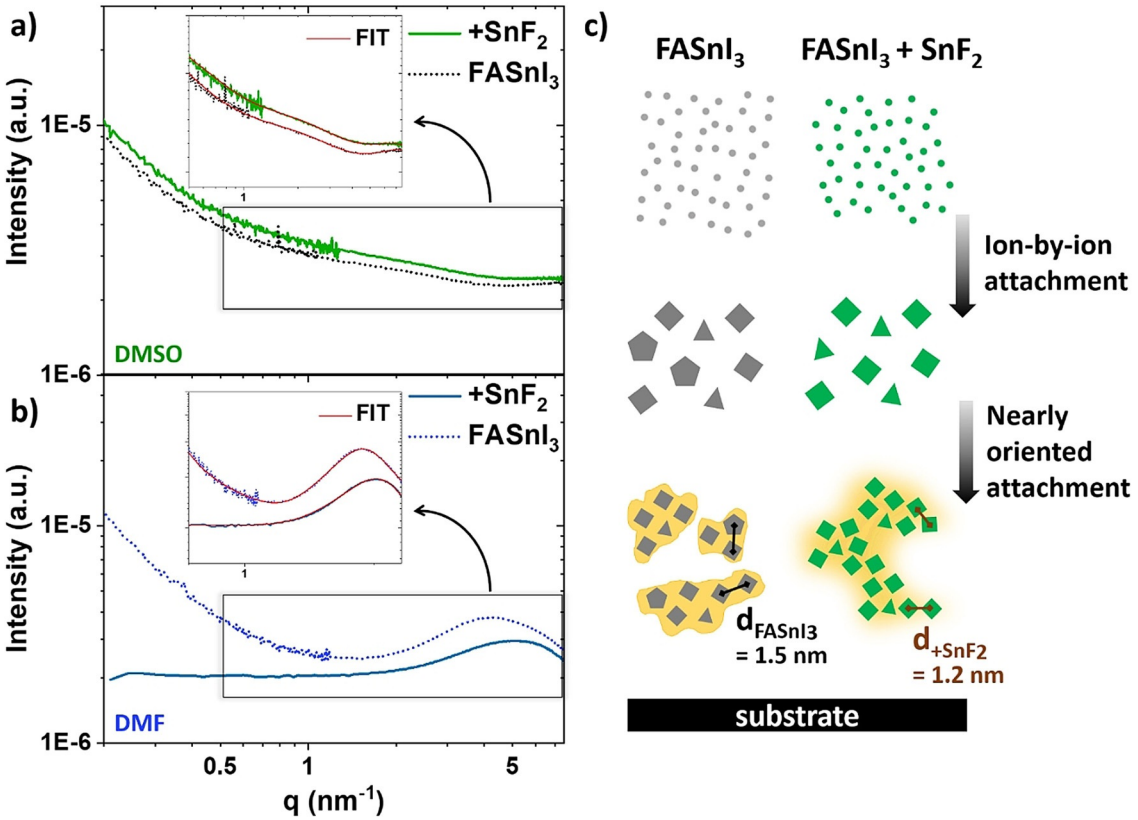


***Figure 4.*** SAXS performed on different $FASnI_3$ precursor solutions. SAXS curves of $FASnI_3$ (dotted line) compared to $FASnI_3$ with $SnF_2$ addition (solid line) in a) DMSO and b) DMF, as well as the corresponding fit given in red in the magnified representations. c) Proposed nucleation and growth mechanism in $FASnI_3$ precursor solution affected by $SnF_2$ addition, where the different forms (triangle, quadrangle, pentagon) should schematically describe the potential variety of subunits.

  

the proximity of interatomic distances. The general behaviour of the initial perovskite precursor stage is highly dependent on the specific solvent environment. Literature shows that solvents with a lower donating number interact weakly, whereas stronger donating solvents interact strongly with the metal of a perovskite precursor solution.[42] Therefore, stronger donating solvents tend to hinder the iodide coordination of the metal. Since DMSO is known to be strongly donating and hence decelerates the perovskite crystallization process, we here include *N*,*N*-dimethylformamide (DMF) with lower donating effect to investigate further the possible influence of $SnF_2$ on the early stages of crystallization. Figure S6 shows the same effect on the color of $SnF_2$ in DMF as in DMSO, as proof that the same visual transformation occurred.

The evolution of a maximum in the SAXS scattering curve of $FASnI_3$ in DMF given in Figure 4b shows a clear difference compared to the scattering curve of pure $FASnI_3$ in DMSO. The maximum emerges based on a dominant structure factor, which evolves due to particle interaction. The mean spacing $d$ between the mass centers of the individual interacting particles can be calculated as discussed by Raghuwanshi et al. using the magnitude of $q$ at the peak maximum.[43] In the plain $FASnI_3$ solution in DMF, this results in a mean spacing $d$ of approximately 1.5 nm. Adding $SnF_2$ to the solution leads to a shift of this peak maximum to higher $q$ and, consequently, lower mean $d$ spacing of 1.2 nm. Besides the shift of the maximum, also the slope at lower $q$-values disappears. The shallow negative slope for both DMF and DMSO solutions gives rise to the presence of larger structures with a broad size distribution ($>100$ nm) in the solution. We propose that the larger sizes represent aggregates consisting of small interacting subunits formed by ion-to-ion attachment. We assign these subunits to particles or clusters in an average dimension of 0.4 nm observed in all scattering curves. In the DMF case, we assume that these aggregates form by nearly oriented attachment, as described in the non-classical nucleation theory being pre-ordered arrangements (Figure 4c).[44–46] The well-pronounced structure factor peak can evidence this, showing the recurring distance $d$ between subunits, representing the average distance between the mass centers of the units and could thus be considered the tin-to-tin distance due to the high electron density of tin. A specific recurring distance $d$ can also be noticed in the case of $SnF_2$ addition. However, there is no negative slope at low $q$-values assigned to larger higher-level structures. Therefore, we conclude that the total size distribution generally appears to be more homogeneous; the nearly oriented attachment with the recurring distance $d$ of 1.2 nm might be considerably more extensive than in the plain $FASnI_3$ solution or even of infinite size. Additionally, we performed several runs for every sample to prove no damage caused by the beam (Figure S7).

Pre-ordered arrangements of subunits set the starting point for the further crystallization of a thin film on a substrate. The broad size distribution of comparable smaller aggregates might result in films including unordered pores or pinholes because solvent evaporation leaves holes between the pre-ordered totals. Instead, the more uniform size distribution due to a larger oriented attachment of the subunits supports homogeneously distributed crystal growth, a suitable substrate coverage and improved film morphology, precisely what is observed by $SnF_2$ addition in literature.[22,25,28] With the premise of the already advanced aggregation of elements in the DMF solvent, a similar mechanism during the late stages of enhanced crystallization may be expected for the case of DMSO. By applying pressure via spin coating and solvent evaporation, the concentration of $FASnI_3$ in the solution increases. Following the evolution of SAXS scattering curves for $FASnI_3$ concentration series in DMF and DMSO, it suggests that a structure factor maximum is formed at higher concentrations in the case of DMSO comparable to the DMF solution (Figure S8). In this sense, the observed behaviour for DMF can be extrapolated to a more advanced stage of precursor formation for the DMSO precursor solution. Therefore, $SnF_2$ as an additive leads to an in total more homogeneous crystallization of the tin halide perovskite thin film, and thus to a better morphology.

Regarding the change in solution color caused by $SnF_2$ addition, we speculate that fluoride modifies the coordination level of tin centers by iodide ions, hindering the formation of colorful, highly coordinated $[SnI_x]^{2-x}$ units. The fact that better morphology films are obtained through the pale yellow, $SnF_2$-containing solution points out that, with solution color as an indication, the properties of the existing formations in solution critically influence the crystallization dynamics of tin halide perovskites. This feature is currently underexplored for these materials and proves to be much more complex and sensitive than for their lead analogues due to its quite restricted processing conditions.

Other $SnX_2$ ($X = Cl$, Br, I) and their influence on perovskite properties are also frequently discussed in the literature.[16,17,47] We further performed SAXS on $FASnI_3$ precursor solutions according to $SnX_2$ addition, given in Figure S9, to compare their respective functionality to the $SnF_2$ addition. Similar to the scattering curves shown in Figure 4a, no significant influence or difference between different X can be noted. However, it should not be ruled out that they could have the same behavior difference as $SnF_2$ in other solvents like DMSO and DMF. This confirms the need to investigate the strong dependence of additives and compositions used for tin halide perovskites. Finally, a scattering curve for the presence of $Sn^{IV}$ is given in the inset window in Figure S9, for which we measured an aged sample of $FASnI_3$. The effect of temperature-induced degradation of DMSO solutions on its properties seems relevant, confirming that we did not influence unexpected $Sn^{IV}$ content in $FASnI_3$ with or without $SnX_2$.

Although SAXS detected no difference for the different $SnX_2$ additives in DMSO solutions, they still caused a color change in a clear trend (Figure 5a). Both $SnF_2$ and $SnCl_2$ led to a similar yellow coloration of $FASnI_3$ solution, while $SnBr_2$ affected it mildly more. This trend could mean that the colorful, highly coordinated $[SnI_x]^{2-x}$ iodostannates were hindered more strongly as the halide X is a harder Lewis base. The fresh solutions were analyzed by $^{119}$Sn-NMR (Figure S10), although no notable difference was found except for the shielding effect from $SnF_2$, already discussed in Figure 2. In this sense, $SnF_2$ is the only $SnX_2$ additive

  

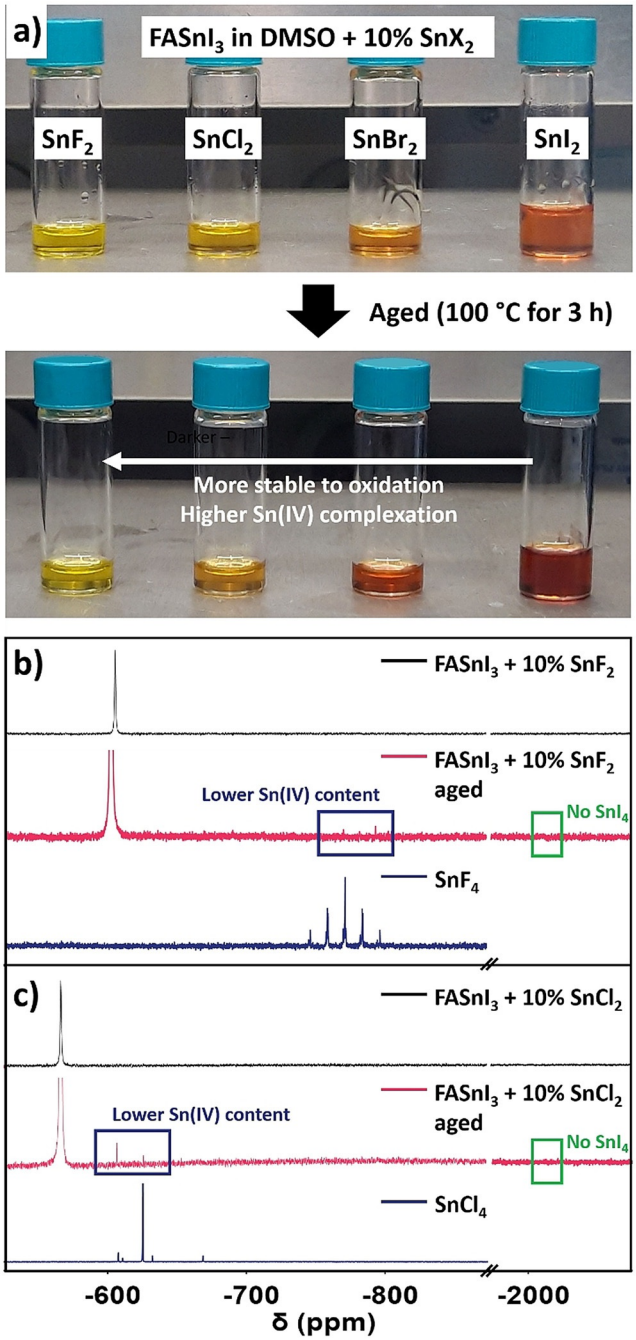


***Figure 5.*** a) Fresh and aged solutions of $FASnI_3$ in DMSO with 10% $SnF_2$, $SnCl_2$, $SnBr_2$ and $SnI_2$. An arrow points out the difference in darkening as an effect of the ageing treatment. $^{119}$Sn-NMR spectra of b) 10% $SnF_2$- and c) 10% $SnCl_2$-containing $FASnI_3$ solution before and after being aged. $SnF_4$ and $SnCl_4$ solutions spectra are added as indicative of the species formed under the ageing process.

shifting the $FASnI_3$ signal upfield, while $SnCl_2$ and $SnBr_2$ go slightly in the opposite direction. This effect correlates well with the chemical shifts in the different $SnX_2$-pure solutions in DMSO (Figure S11), except for the $SnI_2$ case. Hence, the final $Sn^{II}$ signal position might be an average value of all $Sn^{II}$ species. After heating the solutions, we observed that the solution's darkening was negligible for chloride- and fluoride-containing solutions, which could be due to both lower $Sn^{II}$ oxidation and more efficient $Sn^{IV}$ complexation by these anions, as explained in Figure 2. The heated solutions were measured by $^{119}$Sn-NMR (Figure 5b), showing that the content of $Sn^{IV}$, all in the form of $SnF_4$, had been significantly reduced in comparison to $SnF_2$-free heated solution (Figure 2c). We hypothesize that fluoride could affect DMSO and $Sn^{II}$ environments, maybe through the modulation of $[SnI_x]^{2-x}$ adducts, making these two species less eager to undergo a redox reaction. Also, we observed that $SnCl_2$ addition had the same effect as $SnF_2$, leading to both reduction of the oxidation and the selective complexation of $Sn^{IV}$ through the formation of $SnCl_4$ (Figure 5c). These results prove that hard Lewis bases like chloride and fluoride can block the formation of $Sn^{IV}$ in the solution and their introduction into the perovskite film through two different mechanisms: complexation of $Sn^{IV}$ and antioxidative character. Our findings agree with previous reports on reducing $Sn^{IV}$ by the addition of $SnF_2$[23,28,30] or $SnCl_2$[16,17] and suggest that many of the other additives employed in literature for tin halide perovskites may work in the same fashion.

To confirm that fluoride was responsible for these changes in solution, we prepared $FASnI_3$ solutions containing other fluoride-based compounds. Unfortunately, other common species (i.e. CsF and NaF) had limited solubility in common solvents. Therefore we had to saturate the $FASnI_3$ solution below a 5% molar ratio (Figure S12). Even though the concentration was lower than for $SnF_2$, we observed the exact change in color from orange to pale yellow, potentially affecting perovskite subunits in solution in the same fashion. Similarly, these solutions experienced no darkening of solutions aged at 100 °C for 3 h in different conditions, proving the complexation of $Sn^{IV}$ in the form of $SnF_4$. Even though these particular additives may not be directly implementable due to the strong influence that $Cs^+$ and $Na^+$ cations can have in the perovskite solar cells processing and performance, these results confirm the universality of the working principle for fluoride-based compounds. Furthermore, they suggest that $SnF_2$ additive may be eventually replaceable by other fluoride-based species if applied in the right conditions.

To complete the study, we wanted to investigate how these changes in perovskite solution properties affect the thin film formation and the corresponding solar cells performance. We fabricated pristine $FASnI_3$ films and with 10% of the excess of FAI, $SnI_2$, $SnBr_2$, $SnCl_2$ and $SnF_2$. Excess FAI was tried to study both stoichiometry sides of $FASnI_3$. While there was no notable change in the X-ray diffraction patterns (Figure S13), the scanning electron microscopy (SEM) results offered some differences among samples (Figure S14). The sample with 10% $SnI_2$ excess was the only one showing a high density of extensive pinholes. In contrast, the film with 10% $SnF_2$ was the most homogeneous one, free of pinholes and other minor irregularities that are present in the rest of the films, agreeing with previous papers that used $SnF_2$ on its beneficial effect on morphology.[22,25,28]

There is an evident change in the resulting grain size with the changing halide element (Figure S15). Fluoride led to the smallest average grain size (568 nm) compared to chloride (629 nm) and bromide (623 nm). These results are orthogonal

  

to those reported previously, where fluoride[25] and chloride[17] were said to increase the perovskite crystals' grain size. However, tin halide perovskites' sensitive nature implies that significant changes can be expected from minor modifications in the perovskite composition or processing. Therefore, the effect of halides introduction can vary from study to study. Also, stoichiometry in pure $FASnI_3$ perovskite strongly affects the pinhole density and the average grain size. The largest size was found for equimolar $FASnI_3$ (695 nm), which went down when increasing or decreasing the $SnI_2$ ratio (647 and 568 nm, respectively). Moreover, $SnF_2$ addition shows an impact on the size distribution itself, which is significantly narrowed to plain $FASnI_3$ thin film. These observations agree with the results by SAXS, assuming that a uniformly nearly oriented attachment in solution leads to a more homogeneous distribution of the grain sizes in the film.

We then used these films for solar cells fabrication (more details in the Supporting Information) to investigate any possible trend between additives and performance. In this sense, adding a small portion of tin halides to $FASnI_3$ solutions seems beneficial for the device performance, showing some positive trend when moving to lower size halides (Figure S16). Though it appears that smaller halides—harder Lewis bases—work better by having a more decisive influence in the processing, chloride was the exception. Even though NMR and SAXS found $SnCl_2$ to have very similar behavior to $SnF_2$, the resulting devices yielded no efficiency, suggesting that chloride brings other factors into play. Previous works point out how chloride can be incorporated in the lattice and its tendency to form massive aggregates,[16,17] making its application not as trivial as $SnF_2$ and requiring a more careful optimization. We suspect $SnCl_2$ could mimic $SnF_2$ to some extent in these solutions if the processing conditions are adjusted accordingly. It is also worth noting the slight improvement in efficiency produced just by using a 1,1:1 $SnI_2$:FAI stoichiometry (i.e. 10% $SnI_2$ excess), despite the content of irregularly sized pores (Figure S14). This matches well with the results in previous works,[11,32] proving the importance of providing a Sn-rich environment in the film.

## Conclusion

$SnF_2$ is a widely used additive for tin and lead/tin halide perovskites, systematically showing the same beneficial effects in all reported studies: perovskite films with lower $Sn^{IV}$ content and improved morphology. We uncovered the different roles of fluoride in $SnF_2$ on $Sn^{IV}$ complexation and colloidal arrangement in the precursor solution. By studying the fluoride chemistry in perovskite solutions and films with different complementary techniques, we demonstrated that the fluoride in $SnF_2$ has a critical role in reducing $Sn^{IV}$ content in the precursor solution and the final perovskite film. We showed by NMR the selective complexation of $Sn^{IV}$ in the form of $SnF_4$, which HAXPES revealed to have a lower tendency to get introduced in the film than $SnI_4$. Moreover, we showed how the introduction of $SnF_2$ in perovskite solutions increases their stability against the oxidation caused by DMSO. This antioxidative character was also found for $SnCl_2$, meaning that many other reported additives for tin halide perovskites may also block $Sn^{II}$ oxidation by simple tuning of solution properties. Apart from reducing $Sn^{IV}$ content in the thin film, SAXS measurements on the related precursor solutions evidenced that fluoride alters the essential formation of pre-organized perovskite clusters. We identified an advanced colloidal arrangement in DMF compared to the DMSO solutions that are notably influenced by the addition of $SnF_2$. We assigned this arrangement to an advanced nucleation process in DMF compared to DMSO. Finally, based on our findings, we proposed a nucleation mechanism that occurs in solution and is affected by the $SnF_2$ addition resulting in improved overall crystal quality. In this sense, the effect of $SnF_2$ on the film processing will be strongly determined by the environment in which it is applied (i.e. solvent, perovskite composition). Consequently, there is an immediate need to fundamentally understand and optimize solution properties, their processing and studying the effect of additives. As we are doing in this study with the example of $SnF_2$ as pioneering work and impulse for further research. Overall, we presented a complete comprehensive picture of the working mechanism of $SnF_2$ in tin halide perovskites processing and provided the community with the guidelines for finding new additives with specific chemical properties to selectively complex $Sn^{IV}$ species and regulate the crystallization.

## Acknowledgements

The authors thank HZB for the allocation of synchrotron radiation beamtime for HAXPES experiments. We like to thank the PTB for the ability to use their facilities at BESSY II to carry out SAXS measurements. Further, we acknowledge Uwe Keiderling for providing a suitable software for data treatment. M.F. acknowledges the PhD program of University of Potsdam. G.L. would like to acknowledge China Scholarship Council (CSC) for financial support (Grant No. 201906150131). The authors acknowledge the support of the joint Research School HyPerCells of Helmholtz-Zentrum Berlin and University of Potsdam. Open access funding enabled and organized by Projekt DEAL.

## Conflict of Interest

The authors declare no conflict of interest.

**Keywords:** lead-free systems · perovskite solar cells · tin fluoride · tin halide perovskites · tin oxidation

[1] Best Research-Cell Efficiencies. NREL, accessed May 8, 2021.
[2] J. Li, H.-L. Cao, W.-B. Jiao, Q. Wang, M. Wei, I. Cantone, J. Lü, A. Abate, *Nat. Commun.* **2020**, *11*, 310.
[3] A. Abate, *Joule* **2017**, *1*, 659–664.
[4] X. Jiang, Z. Zang, Y. Zhou, H. Li, Q. Wei, Z. Ning, *Acc. Mater. Res.* **2021**, *2*, 210–219.
[5] G. Nasti, A. Abate, *Adv. Energy Mater.* **2020**, *10*, 1902467.

  

[6] M. Konstantakou, T. Stergiopoulos, *J. Mater. Chem. A* **2017**, *5*, 11518 – 11549.
[7] M. I. Saidaminov, I. Spanopoulos, J. Abed, W. Ke, J. Wicks, M. G. Kanatzidis, E. H. Sargent, *ACS Energy Lett.* **2020**, *5*, 1153 – 1155.
[8] J. Pascual, G. Nasti, M. H. Aldamasy, J. A. Smith, M. Flatken, N. Phung, D. Di Girolamo, S.-H. Turren-Cruz, M. Li, A. Dallmann, R. Avolio, A. Abate, *Mater. Adv.* **2020**, *1*, 1066 – 1070.
[9] X. He, T. Wu, S. Liu, Y. Wang, X. Meng, J. Wu, T. Noda, X. Yang, Y. Moritomo, H. Segawa, L. Han, *J. Mater. Chem. A* **2020**, *8*, 2760 – 2768.
[10] D. Ricciarelli, D. Meggiolaro, F. Ambrosio, F. De Angelis, *ACS Energy Lett.* **2020**, *5*, 2787 – 2795.
[11] D. Di Girolamo, J. Pascual, M. H. Aldamasy, Z. Iqbal, G. Li, E. Radicchi, M. Li, S.-H. Turren-Cruz, G. Nasti, A. Dallmann, F. De Angelis, A. Abate, *ACS Energy Lett.* **2021**, *6*, 959 – 968.
[12] F. Gu, S. Ye, Z. Zhao, H. Rao, Z. Liu, Z. Bian, C. Huang, *Sol. RRL* **2018**, *2*, 1800136.
[13] W. Li, J. Li, J. Li, J. Fan, Y. Mai, L. Wang, *J. Mater. Chem. A* **2016**, *4*, 17104 – 17110.
[14] S. Gupta, D. Cahen, G. Hodes, *J. Phys. Chem. C* **2018**, *122*, 13926 – 13936.
[15] M. H. Kumar, S. Dharani, W. L. Leong, P. P. Boix, R. R. Prabhakar, T. Baikie, C. Shi, H. Ding, R. Ramesh, M. Asta, M. Graetzel, S. G. Mhaisalkar, N. Mathews, *Adv. Mater.* **2014**, *26*, 7122 – 7127.
[16] K. P. Marshall, M. Walker, R. I. Walton, R. A. Hatton, *Nat. Energy* **2016**, *1*, 16178.
[17] Q. Tai, X. Guo, G. Tang, P. You, T.-W. Ng, D. Shen, J. Cao, C.-K. Liu, N. Wang, Y. Zhu, C.-S. Lee, F. Yan, *Angew. Chem. Int. Ed.* **2019**, *58*, 806 – 810; *Angew. Chem.* **2019**, *131*, 816 – 820.
[18] Y. Liao, H. Liu, W. Zhou, D. Yang, Y. Shang, Z. Shi, B. Li, X. Jiang, L. Zhang, L. N. Quan, R. Quintero-Bermudez, B. R. Sutherland, Q. Mi, E. H. Sargent, Z. Ning, *J. Am. Chem. Soc.* **2017**, *139*, 6693 – 6699.
[19] S. Shao, J. Liu, G. Portale, H.-H. Fang, G. R. Blake, G. H. ten Brink, L. J. A. Koster, M. A. Loi, *Adv. Energy Mater.* **2018**, *8*, 1702019.
[20] M. Li, W.-W. Zuo, Y.-G. Yang, M. H. Aldamasy, Q. Wang, S.-H. Turren-Cruz, S.-L. Feng, M. Saliba, Z.-K. Wang, A. Abate, *ACS Energy Lett.* **2020**, *5*, 1923 – 1929.
[21] D. Sabba, H. K. Mulmudi, R. R. Prabhakar, T. Krishnamoorthy, T. Baikie, P. P. Boix, S. Mhaisalkar, N. Mathews, *J. Phys. Chem. C* **2015**, *119*, 1763 – 1767.
[22] W. Liao, D. Zhao, Y. Yu, C. R. Grice, C. Wang, A. J. Cimaroli, P. Schulz, W. Meng, K. Zhu, R.-G. Xiong, Y. Yan, *Adv. Mater.* **2016**, *28*, 9333 – 9340.
[23] S. Gupta, T. Bendikov, G. Hodes, D. Cahen, *ACS Energy Lett.* **2016**, *1*, 1028 – 1033.
[24] T. Handa, T. Yamada, H. Kubota, S. Ise, Y. Miyamoto, Y. Kanemitsu, *J. Phys. Chem. C* **2017**, *121*, 16158 – 16165.
[25] Z. Zhao, F. Gu, Y. Li, W. Sun, S. Ye, H. Rao, Z. Liu, Z. Bian, C. Huang, *Adv. Sci.* **2017**, *4*, 1700204.
[26] S. J. Lee, S. S. Shin, J. Im, T. K. Ahn, J. H. Noh, N. J. Jeon, S. I. Seok, J. Seo, *ACS Energy Lett.* **2018**, *3*, 46 – 53.
[27] S. Gupta, G. Hodes, *SN Appl. Sci.* **2019**, *1*, 1066.
[28] T. M. Koh, T. Krishnamoorthy, N. Yantara, C. Shi, W. L. Leong, P. P. Boix, A. C. Grimsdale, S. G. Mhaisalkar, N. Mathews, *J. Mater. Chem. A* **2015**, *3*, 14996.
[29] R. L. Milot, M. T. Klug, C. L. Davies, Z. Wang, H. Kraus, H. J. Snaith, M. B. Johnston, L. M. Herz, *Adv. Mater.* **2018**, *30*, 1804506.
[30] C. Hartmann, S. Gupta, T. Bendikov, X. Kozina, T. Kunze, R. Félix, G. Hodes, R. G. Wilks, D. Cahen, M. Bär, *ACS Appl. Mater. Interfaces* **2020**, *12*, 12353 – 12361.
[31] T. Yokoyama, T. B. Song, D. H. Cao, C. C. Stoumpos, S. Aramaki, M. G. Kanatzidis, *ACS Energy Lett.* **2017**, *2*, 22 – 28.
[32] K. P. Marshall, R. I. Walton, R. A. Hatton, *J. Mater. Chem. A* **2015**, *3*, 11631 – 11640.
[33] N. Li, S. Tao, Y. Chen, X. Niu, C. K. Onwudinanti, C. Hu, Z. Qiu, Z. Xu, G. Zheng, L. Wang, Y. Zhang, L. Li, H. Liu, Y. Lun, J. Hong, X. Wang, Y. Liu, H. Xie, Y. Gao, Y. Bai, S. Yang, G. Brocks, Q. Chen, H. Zhou, *Nat. Energy* **2019**, *4*, 408 – 415.
[34] T. Nakamura, S. Yakumaru, M. A. Truong, K. Kim, J. Liu, S. Hu, K. Otsuka, R. Hashimoto, R. Murdey, T. Sasamori, H. D. Kim, H. Ohkita, T. Handa, Y. Kanemitsu, A. Wakamiya, *Nat. Commun.* **2020**, *11*, 3008.
[35] T. Birchall, G. Dénès, *Can. J. Chem.* **1984**, *62*, 591 – 595.
[36] L. Lanzetta, T. Webb, N. Zibouche, X. Liang, D. Ding, G. Min, R. J. E. Westbrook, B. Gaggio, T. J. Macdonald, M. S. Islam, S. A. Haque, *Nat. Commun.* **2021**, *12*, 2853.
[37] M. A. Stranick, A. Moskwa, *Surf. Sci. Spectra* **1993**, *2*, 45.
[38] S. Hoste, H. Willeman, D. Van De Vondel, G. P. Van Der Kelen, *J. Electron Spectrosc. Relat. Phenom.* **1974**, *5*, 227.
[39] M. M. S. Karim, A. M. Ganose, L. Pieters, W. W. W. Leung, J. Wade, L. Zhang, D. O. Scanlon, R. G. Palgrave, *Chem. Mater.* **2019**, *31*, 9430.
[40] P. De Padova, M. Fanfoni, R. Larciprete, M. Mangiantini, S. Priori, P. Perfetti, *Surf. Sci.* **1994**, *313*, 379.
[41] I. Breßler, J. Kohlbrecher, A. F. Thünemann, *J. Appl. Crystallogr.* **2015**, *48*, 1587 – 1598.
[42] J. C. Hamill, J. Schwartz, Y. L. Loo, *ACS Energy Lett.* **2018**, *3*, 92 – 97.
[43] V. S. Raghuwanshi, M. Ochmann, A. Hoell, F. Polzer, K. Rademann, *Langmuir* **2014**, *30*, 6038.
[44] M. Niederberger, H. Cölfen, *Phys. Chem. Chem. Phys.* **2006**, *8*, 3271 – 3287.
[45] Y. Liu, H. Geng, X. Qin, Y. Yang, Z. Zeng, S. Chen, Y. Lin, H. Xin, C. Song, X. Zhu, D. Li, J. Zhang, L. Song, Z. Dai, Y. Kawazoe, *Matter* **2019**, *1*, 690 – 704.
[46] J. J. De Yoreo, P. U. P. A. Gilbert, N. A. J. M. Sommerdijk, R. L. Penn, S. Whitelam, D. Joester, H. Zhang, J. D. Rimer, A. Navrotsky, J. F. Banfield, A. F. Wallace, F. M. Michel, F. C. Meldrum, H. Cölfen, P. M. Dove, *Science* **2015**, *349*, aaa6760.
[47] J. H. Heo, J. Kim, H. Kim, S. H. Moon, S. H. Im, K. H. Hong, *J. Phys. Chem. Lett.* **2018**, *9*, 6024 – 6031.

Manuscript received: June 7, 2021
Accepted manuscript online: July 6, 2021
Version of record online: July 24, 2021

  